Geographical Patterning of Interannual Rainfall Variability in the Tropics and Near Tropics: An L-Moments Approach

ROBERT E. DEWAR

Department of Anthropology, University of Connecticut, Storrs, Connecticut

JAMES R. WALLIS

School of Forestry and Environmental Science, Yale University, New Haven, Connecticut

(Manuscript received 2 February 1998, in final form 9 February 1999)

ABSTRACT

Interannual rainfall variability has important effects for the evolution of biotic and human communities. Historical records of monthly rainfall totals for 1492 stations within 30° of the equator were analyzed using the method of L-moments. The 0.1 quantile (QU_{10}), or the proportion of mean annual rainfall expected in the driest year in 10, was selected as the measure of variability. A nonlinear regression was fit to the relationship between QU_{10} and mean annual rainfall, and regions were categorized into three classes on the basis of the residuals: the 25% with the most negative, the 25% with the most positive, and the middle 50%. Maps of the global and regional patterns of rainfall variability show marked geographical patterning of variability and identify areas where rainfall variability may be a particularly important environmental feature.

1. Introduction

Mean annual rainfall has long been known as an important determinant of biological productivity and has been incorporated, in one fashion or another, into almost all classifications of world climate. Modern ecological theory suggests, however, that climatic variability, including rainfall variability, should play a major role in the evolution of life histories of plants and animals (e.g., Schaffer 1974; Stearns 1976; Tuljapurkar 1989). Life histories of species in regions of greater variability can be expected to differ from those in regions of similar annual rainfall, but lower variability. In a pioneering study, Conrad (1941) demonstrated that interannual variability increases as mean annual rainfall declines. In addition, he showed that regions of equivalent mean rainfall may differ significantly in year-to-year variation in total rainfall, and provided a global map of variation in variability. Nicholls (1988) showed, using Conrad's data, that rainfall stations in regions affected by Southern Oscillation events had higher rainfall variability than other stations. Nicholls and Wong (1990) extended these results, using a different and larger dataset, and showed that variability of annual rainfall increases as 1) mean annual rainfall decreases, 2) as latitude decreases, and 3) in tropical and near-tropical regions, as the influence of the Southern Oscillation increases. The present paper seeks to establish more precise mapping of interannual rainfall variation using a larger dataset and a recently developed method for the analysis of regional frequency data (Hosking and Wallis 1997) for those areas within 30° of the equator. The pattern of relative variability offers scientists the opportunity to identify regions where interannual rainfall variability may have been important in the evolution of natural and human communities.

The examination of interannual rainfall variation is fraught with difficulties, both in terms of data and of statistical analysis. In terms of data, two problems are paramount: historical records are available for a very uneven distribution of stations, and even the most carefully compiled datasets suffer from problems of missing data, transcription errors, and unidentified changes in station location and recording method over time. From a statistical point of view, the primary problem is that the distribution of rainfall totals for any given station is very unlikely to be normally distributed. The stations used here varied extensively in the skewness and kurtosis of their recorded distributions. In such a context, comparisons based upon a simple measure of spread like the standard deviation are problematic, particularly because the probability of rainfall deficit years is likely to be more important biologically than that of rainfall

Corresponding author address: Dr. Robert E. Dewar, Department of Anthropology, U-176, University of Connecticut, Storrs, CT 06269.
E-mail: dewar@uconnvm.uconn.edu

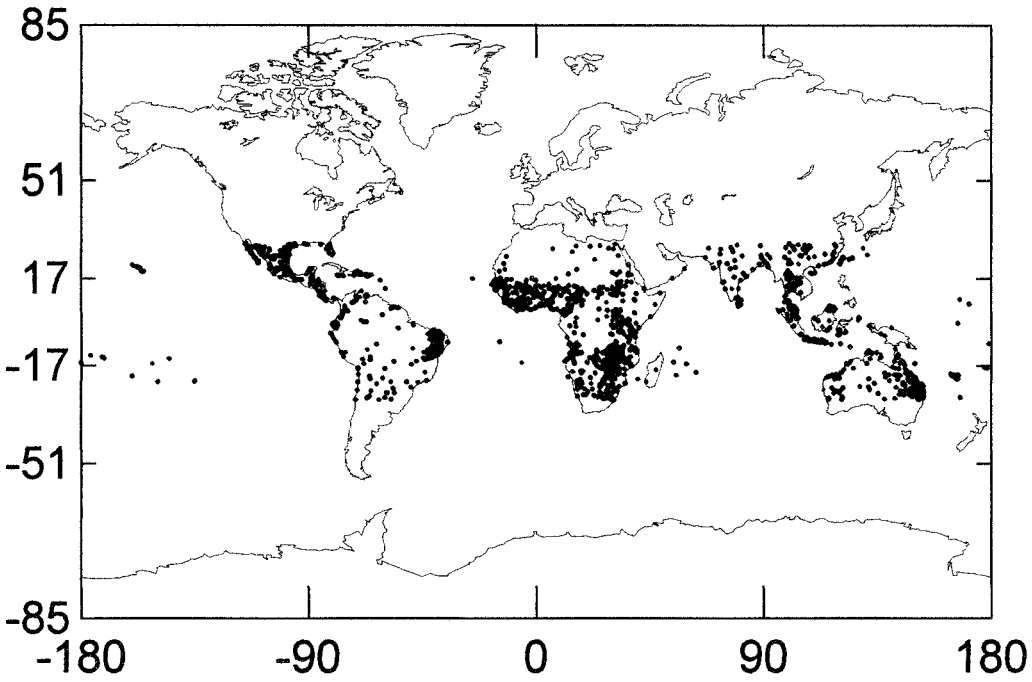

FIG. 1. Precipitation stations retained in the regional analysis.

surpluses. This follows from Liebig's ''law of the minimum'' (1964); biological systems are limited by whichever essential input is in shortest supply, and increases in the availability of nonlimiting factors have little effect on productivity. Even more difficulties arise from extrapolating climatic variability to places where stations are not located. In this analysis, an attempt has been made to limit the impact of each of these problems and to provide a relatively robust description of interannual rainfall variation in the tropical regions.

2. Data and methods

The data used here are derived from the Global Historical Climatology Network (GHCN) datasets (Vose et al. 1992) of monthly precipitation totals and station characteristics. Prior to their release, these data were subjected to a quality control process that included plotting each series to identify gross errors. Nonetheless, the records vary considerably in completeness and record length, and it was necessary to employ some arbitrary initial rules to screen the data, of which a subset was selected for subsequent analysis. First, for pragmatic reasons, and in order to ease interpretation, only stations located between 30°N and 30°S latitude were retained. Second, because substantial numbers of missing data compromise analyses of variation, only stations with less than 5% missing data were retained. Third, in order to limit the impact of long-term secular change, and other deviations from stationarity, only data from January 1940 and after were employed. Finally, only stations that had 20 complete annual records after 1940 were retained. The subset thus selected numbered 1527 stations (Fig. 1), and record lengths ranged from 20 to 49 yr, with a median of 37. It is immediately apparent that there is a far from uniform coverage of the Tropics, and some regions, most particularly South America, have very poor coverage.

One major problem in the analysis of annual rainfall totals can arise from the arbitrary division of years between December and January. This is particularly problematic for stations whose season of highest rainfall occurs in these months, because unusually wet or dry rainy seasons are divided between two years. In order to avoid this problem, mean monthly rainfall was calculated for all stations, and the month with the lowest mean rainfall was selected as the beginning of each station's year. Thus, annual totals are calculated as the sum of the 12 months following the driest month at each station. The GHCN monthly totals are presented in units of tenths of millimeters; when a monthly total was reported as ''trace,'' it was arbitrarily set to 0.1 mm.

For each station, data on latitude, longitude, and elevation were collected from the GHCN dataset; when elevations were missing, they were estimated from the ETOPO-5 elevation dataset (NOAA 1988). In addition, the following characteristics were calculated for each station, using the complete post-1940 records: the beginning month of the 2-month period with the lowest mean rainfall, the mean amount of rain that fell during that period, the beginning month of the 2-month period with the highest mean rainfall, the amount of rain that fell in that period, and the ratio of the minimum average

TABLE 1. Transformations and weighting of site characteristics used in the initial clustering.

Site characteristics	Transformation	Weighting
Lat	Mean = 0, std dev = 1	5
Long	Mean = 0, std dev = 1	5
Elev	Log_{10}, and then mean = 0, std dev = 1	2
Mean annual rainfall	Sq. root, and then mean = 0, std dev = 1	2
Ratio of min average 2-month precipitation to max 2-month precipitation	Sq. root, and then mean = 0, std dev = 1	2
Beginning month of min average 2-month precipitation	$\cos(2\pi$ month/12) and $\sin(2\pi$ month/12), and then each transformed to mean = 0, std dev = 1	1 each
Beginning month of max average 2-month precipitation	$\cos(2\pi$ month/12) and $\sin(2\pi$ month/12), and then each transformed to mean = 0, std dev = 1	1 each

2-month precipitation to the maximum average 2-month precipitation.

The analytic methods follow the model established by Guttman (1993), with some modifications described below. The method proceeds by establishing regions through a cluster analysis of station characteristics other than those directly related to variability, and then testing the regions thus formed with measures of discordancy and heterogeneity based upon the frequency distributions of the clustered stations. When regions are heterogeneous, additional cluster analysis is employed to divide the stations into more homogenous regions. Discrepant stations are examined to see if they can be moved to adjacent clusters, if new clusters can be created that make climatological sense, of if there are clear errors in the data.

The analysis began by the creation of provisional climatic regions by a cluster analysis of site characteristics other than variability, using the cluster analysis programs supplied by Hosking (1997). Seven variables were selected as descriptors of precipitation region. Histograms of three variables suggested that reshaping would be helpful; thus mean annual precipitation and the ratio of minimum average 2-month precipitation to maximum 2-month precipitation were transformed by taking square roots, and elevation was transformed by $\log_{10}$, with an elevation of 1 m substituted for the four stations at sea level, and the single station with a negative elevation (Biwa, Egypt, at −15 m). As suggested by Hosking and Wallis (1997), the months identifying the minimum and maximum 2-month periods of precipitation were replaced by two transformed variables [$\sin(2\pi$ month/12) and $\cos(2\pi$ month/12)]. All of the variables, or their transformations, were standardized to a mean of zero, with a standard deviation of 1. Finally, the variables were multiplicatively weighted, such that half of the overall weight of the variability was due to latitude and longitude, and half was associated with the other five variables. This weighting of locational variables proved necessary to produce clusters of sites that were contiguous in two-dimensional space. Table 1 gives a description of the variables and the transformations employed. The cluster analysis employed Euclidean distances and used an average-linkage algorithm, followed by adjustment with *k*-means clustering. This follows the recommendations of Hosking and Wallis (1997, 59–59) for the formation of clusters for frequency analysis, and we employed the algorithms distributed by Hosking (1997). After some experimentation, a clustering of 50 clusters was selected as a starting point for subsequent analysis. These were inspected for geographical and climatological interpretability, and many were divided.

The moments of the frequency distribution of annual precipitation were estimated for every station using the method of L-moments (Hosking 1990; Hosking and Wallis 1997). The first sample moment (l_1) is equal to the mean annual rainfall. The second sample moment (l_2) is a measure of dispersion (½ of Gini's mean difference) analogous to standard deviation. A dimensionless measure of variability, L-CV, is defined as (l_2/l_1) and is analogous to the more familiar coefficient of variation. L-skewness and L-kurtosis are equally dimensionless and defined as (l_3/l_2) and (l_4/l_2), respectively.

The clusters created were examined for station discordancy, using the measure D_i, and for heterogeneity, using the measure H (Hosking and Wallis 1997, p. 63), as well as subjectively, for geographical and climatological plausibility. The data for discordant stations were examined by plotting time series, and inspecting the data directly. In several cases, stations were dropped from the analysis when the records seemed highly implausible, or when there was a clear indication of error. The most common problems were the result of apparently misplaced decimal points—when a station's average annual precipitation suddenly and permanently increased or decreased by an order of magnitude—or the substitution of zeros for missing records. While this latter problem is not easily detectable in arid sites, in moister regions several suspect cases were identified. In such station's records there is a change from a pattern of frequent missing monthly records, to a pattern of no missing data, but several zero monthly rainfall totals in improbable seasons, or in several consecutive months. These were compared to contemporary records at nearby

TABLE 2. Acceptable fits of distributions to homogeneous regions of two or more stations.

Distribution	No. of regions acceptably fitted
Generalized logistic	87
Generalized extreme value	164
Generalized normal	169
Pearson type III	169
Generalized Pareto	19

stations, and if no further evidence of dramatic climatic disturbance could be found, the station was dropped.

Clusters were adjusted by moving sites from one region to another, by subdivision, by assigning all of the sites of a region to neighboring clusters, by merging clusters, or by additional cluster analysis of selected regions. When additional cluster analyses were employed, the variables used were always a subset of the variables listed in Table 1. In these regional cluster analyses, the variables were restandardized to a mean of 0 and a standard deviation of 1, and careful attention was paid to the topography and climatic regime. For example, an early, but heterogeneous, cluster included lowland sites from the southernmost Malay Peninsula and northern Sumatra. In this area, latitude, longitude, elevation, and mean annual rainfall contributed little variance; the clusters primarily divide on the variables relecting rainfall seasonality, and the final clusters seem to represent the difference between those stations most strongly influenced by the Indian Ocean circulation, and those that faced the East China Sea. At each point, the goal was to find physically plausible regions that were reasonably homogeneous in terms of their frequency distributions. This process continued through several iterations until no further progress seemed likely.

For each region, a goodness of fit statistic Z^{DIST} was calculated for six distributions: generalized logistic, generalized extreme value, lognormal, Pearson type III, generalized Pareto, and Wakeby (Hosking and Wallis 1997). As Table 2 indicates, three distributions performed essentially identically and any of these could have been used. Following Guttman et al. (1993), where a Pearson type III distribution gave an acceptable fit, the quantiles of precipitation were estimated from that distribution. In other cases, the quantiles were calculated from the fitted Wakeby distribution. With five parameters, a Wakeby distribution can represent essentially any distribution. For the two heterogeneous regions, a Wakeby distribution was similarly fitted. In the case of seven regions, the proportions of years of zero precipitation were sufficiently large that negative quantiles resulted. For these regions, a Wakeby distribution with the lower bound constrained to zero for all quantiles less than the proportion of zeros in the regional dataset was fitted (Hosking and Wallis 1997, 176–177).

The quantile 0.10 was selected as a measure of regional variability of interest to ecological studies. It represents the proportion of mean annual rainfall of the driest 10% of years. The selection is arbitrary, but the mapping of variability is very similar if the 0.05 or 0.20 quantiles are used. Variability is highly dependent upon the mean, with arid regions much more variable than wetter regions. This effect was removed by means of a nonlinear regression of the 0.1 quantile against mean rainfall. The equation fitted was $QU_{10} = a + b/(c + \text{mean rainfall})$, where a, b, and c are parameters to be determined. The three parameter fitted equation follows Conrad (1941) and Nichols (1988). The fitting was accomplished with a modified Gauss–Newton algorithm minimizing least squares (Engelman and Wilkinson 1996). Because regions composed of only one or two stations were often outliers, the regression equation was calculated only for regions with at least three stations. The residuals of this regression, which reflect greater or lesser variability of a region in comparison to regions of roughly similar rainfall, were then mapped. The resulting map offers a clear guide to patterns of rainfall variability in the Tropics.

TABLE 3. Distribution of the number of regions by size.

Region size	No. of regions	Cumulative no. of stations
1	49	49
2	36	121
3	34	223
4	23	315
5	17	400
6	16	496
7	17	615
8	18	759
9	8	831
10	3	861
11	6	927
12	6	999
13	4	1051
14	4	1107
15	1	1122
16	3	1170
17	3	1221
18	1	1239
19	1	1258
21	1	1279
25	3	1354
29	1	1383
31	1	1414
38	1	1452
40	1	1492

3. Results

The initial sample of 1527 stations was eventually reduced to 1492, divided among 256 clusters. The clusters varied in size from 1 to 40 stations (see Table 3). Although the reliability of the quantiles fitted to each region increases with the number of stations included, the extremely uneven distribution of stations meant that many stations were geographically isolated, and because of differences of distance, elevation, and relief likely to

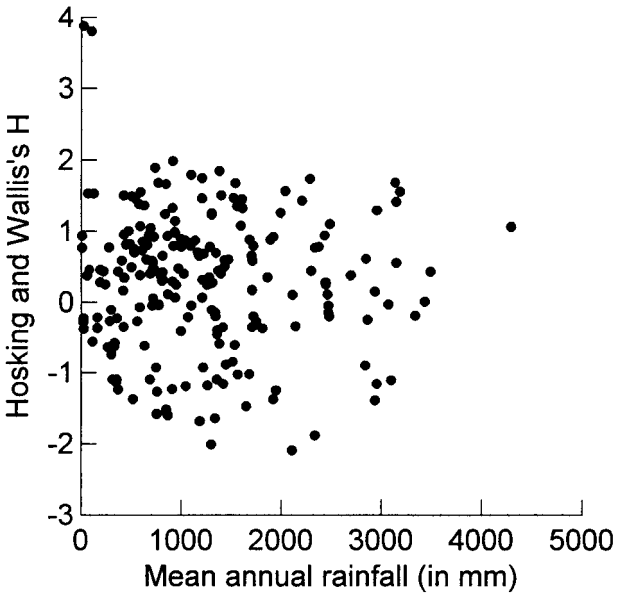

FIG. 2. Heterogeneity of final regions, in comparison to the mean annual rainfall of the regions, weighted by the number of years of record for each station.

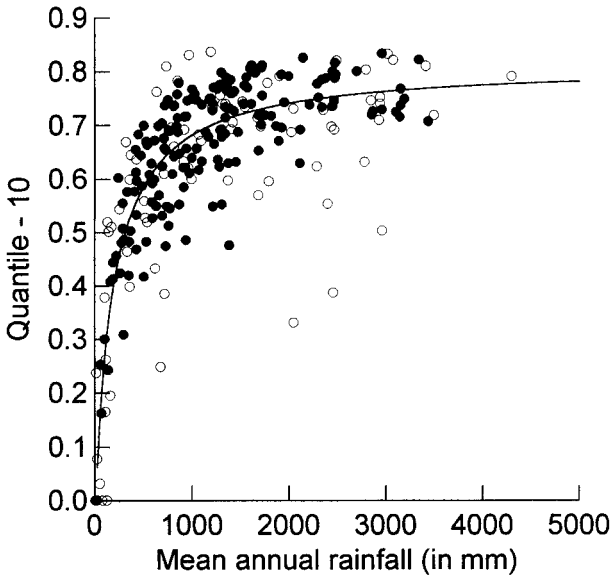

FIG. 3. Nonlinear regression of QU_{10} against weighted mean annual rainfall. The line was fitted only to regions with three or more stations (filled circles), but regions of one or two stations are also located on this graph (open circles).

be climatically divergent from any of the neighboring, but distant, regions. Additional complications arose in areas of extremely high relief, where a high-altitude station may be very different from nearby lower-elevation stations, and on oceanic islands, where a windward station might have very different patterns of rainfall from neighboring leeward stations. In each of these kinds of cases, genuine climatic differences isolated the stations from neighboring regions. In all cases, stations placed in a cluster of their own for reasons of distant location or divergent climatic character as reflected in the variables of Table 1. Sites were not isolated solely because of differences in rainfall variability.

Of the 209 regions with two or more stations, only two remained definitely heterogeneous ($H > 2.0$). Both of these regions were extremely arid (see Fig. 2), with stations characterized by very high L-CV values. The first was a region of six stations, located along the northern and central coast of Peru. The weighted mean annual rainfall total for this region was 2 cm of rain per year. The other was a region of three stations in the lowland interior of Baja California, with a weighted mean annual rainfall of 13 cm. In the Peruvian records, many years saw no rain at all, and in Baja California, rainfall is sporadic. In such circumstances, the annual total of rainfall is the product of very rare events; reliable estimates of the moments of the frequency distribution of such low frequency events may require longer records than were used in this study.

The equation fit to the relationship of QU_{10} to mean annual rainfall for homogeneous regions with at least three stations is

$$QU_{10} = 0.813 + -154.6/(180.8 + WTM),$$

where WTM is the regional mean annual rainfall in millimeters, weighted for record length. The relationship is strong (corrected $r^2 = 0.79$) and Fig. 3 shows the fitted line in relation to all 258 regions. Residuals of predicted–estimated QU_{10} were calculated for all 258 regions. We chose to fit our equation against mean, rather than median, rainfall totals simply because mean annual rainfall is far more commonly reported.

The distribution of regional residuals was arbitrarily sliced at the hinges of the distribution, yielding three classes of regions: the lowest and highest quartiles, and the middle 50%. The lowest quartile thus represents those regions where the driest year in 10 is drier than expected for regions of similar rainfall, and the highest quartiles are those where the driest year in 10 is less different than expected. This division of the regions is arbitrary, but it has the advantage of being relatively robust to the presence of outliers. Conrad (1941) mapped variability with zero isonomals—lines that divide stations with more from stations with less variability than expected, but usually without indication of the magnitude of the difference. In four cases, he indicated areas of especially marked variability: Malden Island, northeastern Brazil, coastal Peru and Chile, and an area stretching from northwestern India through Saudi Arabia to Ethiopia. While our analyses show the first two cases as parts of highly variable regions, in the latter two cases our mapping differs from his: the Peruvian coast does not seem to be more variable than would be expected for such an arid climate, and the Horn of Africa and the northwest Indian subcontinent appear as two smaller, but distinct regions of variability.

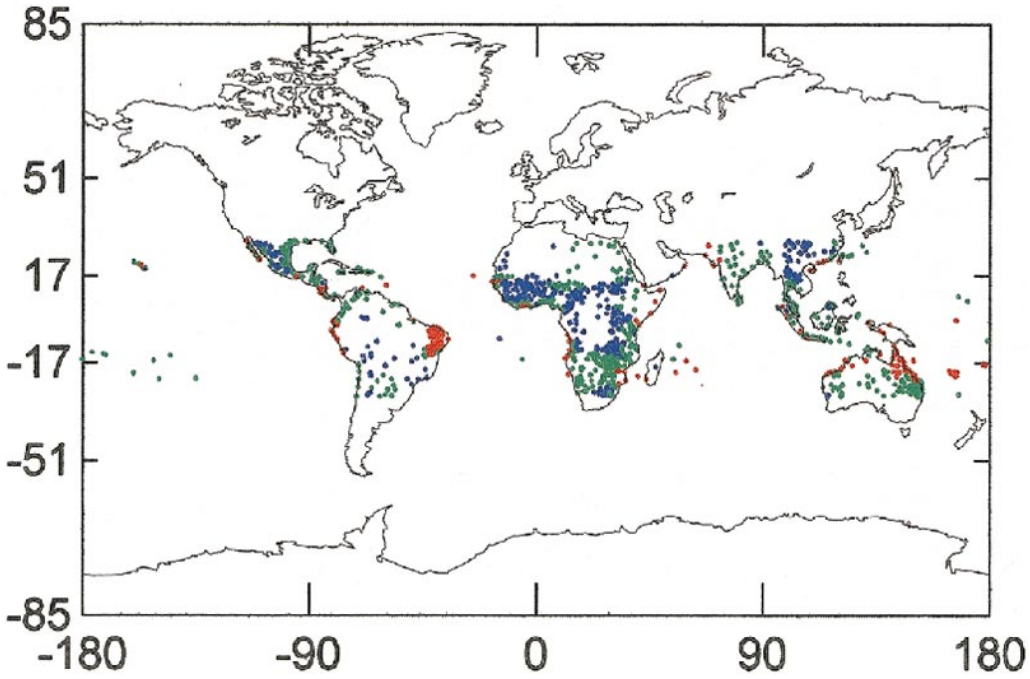

FIG. 4. Variation in the QU_{10} on a global basis. Red dots are the stations from the most variable regions, green are the stations from the middle 50% of regions, and blue are the stations from the least variable regions.

a. Global

The geographical patterning of rainfall data is very striking, and far from random. Figure 4 illustrates the distribution of stations of each of the three classes. Although there are scattered outliers of high variability stations, there is a clear geographical patterning, suggesting that the methods employed reflect underlying climatic reality. One obvious feature is that oceanic islands have a strong tendency toward variability; Ascension, in the South Atlantic, is the only station to fall in the least variable quartile. A second feature of note, which echoes the findings of Conrad (1941), is that most high variability regions are located near coasts, and continental interiors tend to be areas of reduced variability. When clusters of fewer than three stations are excluded as possible outliers, highly variable clusters were compared with clusters of low to moderate variability. Variable clusters were significantly more likely to be south of the equator (Mann–Whitney U test, $p = 0.005$) and have much lower mean elevations ($p = 0.007$) than less variable clusters. They did not vary significantly ($p > 0.1$) in mean annual precipitation or in mean number of stations per cluster.

Ropelewski and Halpert (1987) sought regions of consistent El Niño–Southern Oscillation precipitation patterns around the globe. Their methods focused on establishing areas where they could identify seasons of 4 months or greater where there were coherent and fairly consistent responses to El Niño events. Of the nine tropical regions they identified where an El Niño–related season brought reduced precipitation, we have data for eight (not for their ''Micronesia–W. Pacific'' region), and there are highly variable regions in each. Ropelewski and Halpert's regions vary greatly, however (see below), in the proportion of our clusters that are highly variable. They identified four regions where an El Niño–related season brought increased precipitation; we have data for three (not for their ''Central Pacific'' region), and in none of these are there any highly variable stations.

Examining the question of the strength of the relationship between ENSO events and the patterns of variability presented here is a complex issue, and our discussion is preliminary. To try to make comparisons with Ropelewski and Halpert, who focused their attention only on relatively large regions, we have grouped all of the highly variable clusters with at least three stations into 16 macroregions (see Table 4). In five cases, these macroregions were clearly included in one of Ropelewski and Halpert's regions. The relationship between El Niño and the droughts in Northeast Brazil has been shown to be very weak (Rao et al. 1993; Kane 1997) and was not pursued here. For the remaining nine clusters, we examined the data for all stations in a fashion similar to that employed by Ropelewski and Halpert. The monthly rainfall totals for the complete record for each station were converted to ranks and then percentiles, and then averaged for each month of the 24 months of the ENSO cycle that they employed, that is, from July(−1) to June(+1). The patterns of anomalies for all stations in a cluster were inspected by eye to identify seasons of consistently negative or positive anomalies.

TABLE 4. Macroregions and relationship to seasons of correlated response to El Niño events.

Macroregion	No. of clusters/ no. of stations	R–H region*	Effect	Season	Effect	No. of El Niño yr season anomalies in predicted direction
Baja, Mexico	2/15	—	—	—	—	—
Tehuantepec, Mexico	2/7	—	—	Jul(0)–Sep(0)	Negative	6/8
Nicaragua–Panama	2/6	CEN	Negative			
Peru–Ecuador**	2/10	—	—	Mar(0)–Jun(0)	Positive	13/16
NE Brazil	11/159	—	—			
Senegal	1/11	—	—	—	—	—
Ivory Coast	1/3	—	—	—	—	—
Angola	1/4	—	—	—	—	—
Mozambique–Zimbabwe	2/10	SEA	Negative			
Kenya–Somalia	1/3	—	—	—	—	—
SW Indian Ocean	1/3	—	—	—	—	—
SE China	1/4	—	—	—	—	—
New Guinea	1/4	ING	Negative			
NW Australia	2/9	NAU	Negative			
Queensland	2/9	NAU/EAU	Negative			
New Caledonia	1/14	FNC	Negative			

* From Ropelewski and Halpert (1987).

** Results are for the four stations in the Ecuador cluster; the stations from Peru have far too many months without rainfall to permit analysis.

When candidate seasons were identified, averages of the percentiles for each month in the season and each station were calculated. A Mann–Whitney *U* test was employed to test whether the time- and station-averaged percentiles discriminated ENSO years from non-ENSO years. If they did, time series were plotted to determine the consistency of the ENSO-related pattern. Finally, Spearman rank correlations were examined to determine if the records for each station were positively correlated with the average.

In the end, only two macroregions had clear and consistent seasons of precipitation anomalies. In a macrocluster of seven stations on the west side of the Isthmus of Tehuantepec in Oaxaca, a 3-month season [Jul(0)–Sep(0)] was associated with rainfall deficits and was identifiable in six of eight ENSO cycles. Along the western coast of Peru and Ecuador, a macrocluster of two variable clusters was examined. Here, it was possible to show a clear positive anomaly in a 4-month season [Mar(0)–Jun(0)] identifiable for 13 of 16 ENSO events, for the Ecuadorian cluster only. The Peruvian cluster, is extremely arid (mean annual precipitation <3 cm yr^{-1}), and with the majority of monthly records equaling zero, this kind of analysis proved impossible.

The high variability clusters were then divided into two groups: those from regions that had detectable El Niño–related negative precipitation anomalies, and those that did not, that is, that had no detectable season or that had a season of positive precipitation anomalies. These groups did not differ significantly in terms of mean annual rainfall, the number of stations included in the clusters, or in elevation. They did differ significantly in three ways: the El Niño–related clusters were more likely to be in the Eastern rather than the Western Hemisphere (all are Mann–Whitney *U* tests, $p = 0.020$), they were more likely to be in the Southern Hemisphere ($p = 0.028$), and the El Niño–related clusters were significantly farther from the equator ($p = 0.003$).

The nine macroregions that do not have a clear season of ENSO-related negative precipitation anomalies share few climatic or geographic features as a group. For example, they range from very large areas—as Northeast Brazil—to very small, as Baja, Mexico. It is noteworthy that four of these clusters fall on opposite sides of the Atlantic Ocean. Sea surface temperature anomalies in the tropical Atlantic have been clearly related to drought in Northeast Brazil, and these may be relevant for the clusters in Angola, the Ivory Coast, and Senegal (Rao et al. 1993; Kane 1997). Similarly, three of the clusters are found in the western Indian Ocean and may be responding to a common underlying dynamic.

We conclude from this that a regular pattern of seasons of negative precipitation anomalies associated with ENSO events can contribute to reducing the QU_{10} of annual rainfall in some regions, but other factors are important as well. Our analysis does not permit the conclusion that ENSO-related precipitation anomalies are alone responsible for excessive variability of precipitation in any region.

b. Africa and Arabia

The distribution of stations in Africa is uneven, with Madagascar represented by only two, and with a poor coverage in the Zaire Basin and in the Sahara (see Fig. 5). The patterning of rainfall variability is quite striking, however. Central and Western Africa form a very large region of reduced annual rainfall variation, and in south-

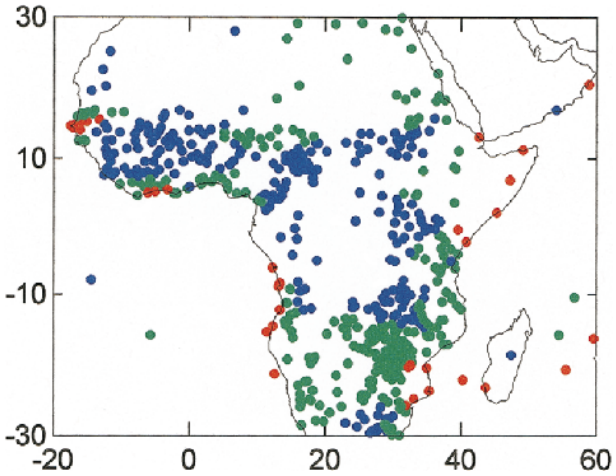

FIG. 5. Variation in the QU_{10} for Africa and Arabia. Red dots are the stations from the most variable regions, green are the stations from the middle 50% of regions, and blue are the stations from the least variable regions.

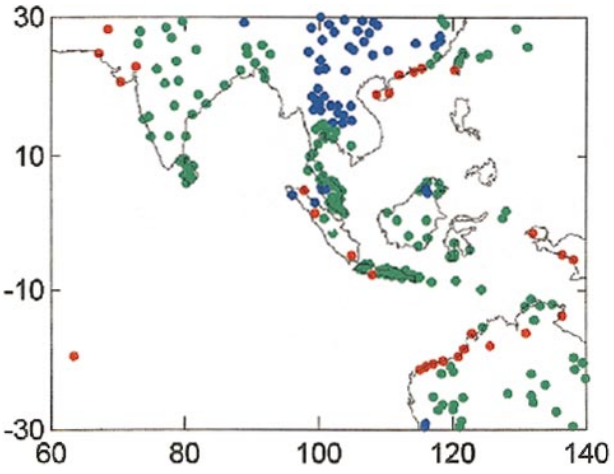

FIG. 6. Variation in the QU_{10} for south and Southeast Asia.

ern Africa there is a similar zone. From roughly the Tropic of Capricorn north to about 15°S there is a zone of moderate variability, which extends northward along the East African rift. The zones of high variability are all much smaller than these features. They are, with rare exceptions, all along or near the coast, and they are to be found in restricted areas of Senegal, the Ivory Coast, Angola and Namibia, and the Somalian and Kenyan coast. There is a larger zone of increased variability that includes the Mascareignes, southern Madagascar, and Mozambique.

Comparison with Ropelewski and Halpert's mapping of ENSO-related precipitation in Africa (1987) yields suggestive relationships. The large area of moderate variability in southern Africa and the more variable region to its east correspond quite well to their ''southeastern Africa region'' where they discovered a consistent decline in rainfall in ENSO years. Their ''equatorial eastern African'' region, roughly centered on Rwanda, Burundi, and Uganda, appears in this analysis to be a zone of reduced severity of the driest year in 10. This makes some sense, since ENSO events tend to bring greater rainfall to this region.

c. South and Southeast Asia

The interior of southern China and northern peninsular Southeast Asia form a zone of reduced variability (see Fig. 6). There is moderate variability from peninsular India through peninsular Thailand and Malaysia and into most of island Southeast Asia, though there are a scatter of stations with greater and lesser variability. There are two compact zones of high variability. The first, stretching from southern Taiwan to Hainan Island, is clearly coastal. The second, in northwestern India and Pakistan, is only in part coastal.

Comparison with Ropelewski and Halpert's maps suggest less concordance than in the case of Africa. Their ''Indian'' region shows a rainfall deficit in ENSO years, but there is no indication of more than moderate variability in the analysis performed here. Nor do they detect an ENSO influence in the region of high variability detected here. On the other hand, their ''Indonesia–New Guinea'' region of ENSO-related precipitation deficit includes all of island Southeast Asia except far northern Sumatra; in our analysis there are a scattering of more variable stations here.

d. Western Pacific

This is clearly a region of relatively high rainfall variability (see Fig. 7). There are very few stations with low variability, and four substantial regions of high variability: 1) coastal northwestern Australia; 2) northern and central Queensland, extending along the coast to the Tropic of Capricorn; 3) Irian Jaya and western Papua

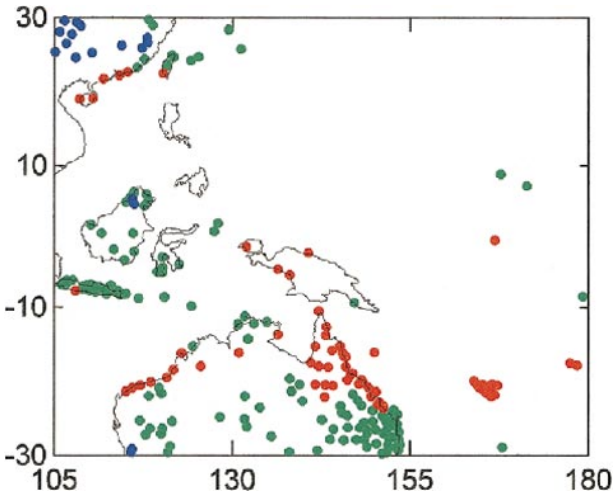

FIG. 7. Variation in the QU_{10} for the western Pacific.

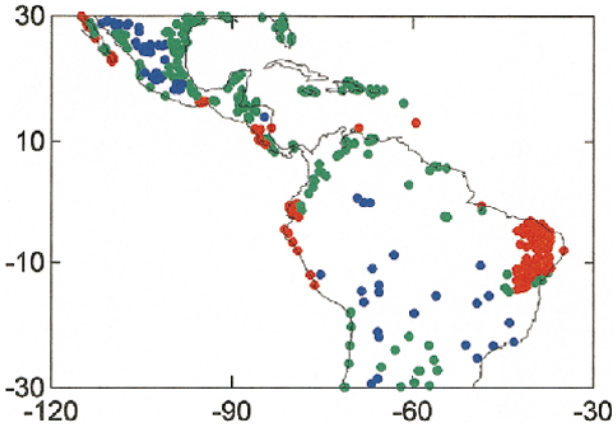

FIG. 8. Variation in the QU_{10} for the tropical New World.

New Guinea, with all stations coastal; and 4) New Caledonia and some nearby oceanic islands. The high variability of this region is not unexpected, since this region has long been described as such. In concordance with the previous regions, there is a tendency for the high variability stations to be along the coasts or on islands. It is important to remember that the contrast between the large area of moderate variability stretching longitudinally across Australia, and the higher variability area of northern Queensland, is one of relative variability, not absolute variability. Central Australia has high variability of annual rainfall, just as almost all arid regions do. Queensland stands out in this analysis for being more variable than other areas with comparable mean annual rainfall.

e. The New World

The pattern in the New World recalls that of Africa more than the western Pacific (see Fig. 8). The continents are, in the interior, fairly uniform in exhibiting low to moderate relative variability. Most coastal zones fall within the moderate class as well. In terms of high variability, there are two patterns, a scattering of small regions in largely coastal zones, and one very compact and very well documented region of northeastern Brazil. Sixty-three percent of all of the stations in this sample from South America are located in northeastern Brazil. This area has long been known to have a highly variable climate, and the extraordinary density of observation stations may be a response to the frequent droughts that occur here. There are seven much smaller zones of high rainfall variability. They include the Baja Californian peninsula, the Isthmus of Tehuantepec, an area of Nicaragua and Panama, a coastal zone of Ecuador and Peru, Curaçao, Barbados, and a single station at the mouth of the Amazon. Ropelewski and Halpert had little data for South America, but there is a fair correspondence between the distribution of more variable stations and their ''Central America and the Caribbean'' zone of reduced precipitation in ENSO years.

4. Summary and conclusions

This study of geographical distribution of variability in the Tropics is the first such effort since that of V. Conrad in 1941. Conrad mapped variability in precipitation for the entire world, using records from 384 stations. For the area between 30°N and 30°S, he had 149 stations. The present study is based upon 10 times as many stations, and thus we are able to characterize the distribution of variability with more precision than Conrad. There remain many areas of the globe where the distribution of stations is quite sparse, and in the future it may be possible to refine the results presented here.

In general, the distribution of high and low variability regions mapped here conform in a general way to both received wisdom, and to the mapping of reduced precipitation teleconnections to ENSO phenomena. Nicholls (1988) has already shown a relationship between rainfall variability and ENSO, in general, so this is not surprising. On the other hand, the maps also identify smaller areas of high variability that are not ENSO related, and for which other explanations must be sought. The most important contribution of these maps is that they are at sufficiently fine a scale to make it possible to identify variability relevant to problems of the ecology and evolution of particular species and human communities. Researchers interested in particular areas will need to seek other sets of rainfall data in order to examine patterns of rainfall variability at a finer scale and with more precision.

Acknowledgments. We would like to thank Alison Richard for perceptive and helpful comments on early drafts of the paper, and Jared Cohon for having introduced us. RED would also like to thank Ronald Smith for encouragement at an early stage in this research.

REFERENCES

Conrad, V., 1941: The variability of precipitation. *Mon. Wea. Rev.*, **69,** 5–11.

Engelman, L., and L. Wilkinson, 1996: Nonlinear regression. *Systat 6.0 for Windows: Statistics,* SPSS, 447–495.

Guttman, N. B., 1993: The use of L-moments in the determination of regional precipitation climates. *J. Climate,* **6,** 2309–2325.

——, J. R. M. Hosking, and J. R. Wallis, 1993: Regional precipitation quantile values for the continental United States computed from L moments. *J. Climate,* **6,** 2326–2340.

Hosking, J. R. M., 1990: L-moments: Analysis and estimation of distributions using linear combinations of order statistics. *J. Roy. Stat. Soc.*, **52B,** 105–124.

——, 1997: Fortran routines for use with the method of L-moments, version 3.02. Research Rep., Research Division, IBM, Yorktown Heights, NY, 33 pp. [Available from IBM Research Division, Thomas J. Watson Research Center, P.O. Box 218, Yorktown Heights, NY 10598.]

——, and J. R. Wallis, 1997: *Regional Frequency Analysis: An Approach Based on L-Moments.* Cambridge University Press, 224 pp.

Kane, R. P., 1997: Prediction of droughts in North-east Brazil: The role of ENSO and use of periodicities. *Int. J. Climatol.*, **17,** 655–665.

Liebig, J. F., 1964: *Animal Chemistry; or, Organic Chemistry in its Application to Physiology and Pathology*. Johnson Reprint Corp. 347 pp. Originally published in 1842.

Nicholls, N., 1988: El Niño–Southern Oscillation and rainfall variability. *J. Climate,* **1,** 418–421.

——, and K. K. Wong, 1990: Dependence of rainfall variability on mean rainfall, latitude, and the Southern Oscillation. *J. Climate,* **3,** 163–170.

NOAA, 1988: Digital relief of the surface of the Earth. Data Announcement 88-MGG-02, National Geophysical Data Center, Boulder, CO. [Available from NOAA/NGDC, Mail Code E/GC3, 325 Broadway, Boulder, CO 80303.]

Rao, U. B., M. C. de Lima, and S. H. Franchito, 1993: Seasonal and interannual variations of rainfall over eastern Northeast Brazil. *J. Climate,* **6,** 1754–1763.

Ropelewski, C. F., and M. S. Halpert, 1987: Global and regional scale precipitation patterns associated with the El Niño Southern Oscillation. *Mon. Wea. Rev.,* **115,** 1606–1626.

Schaffer, W. M., 1974: Optimal reproductive effort in fluctuating environments. *Amer. Nat.,* **108,** 783–790.

Stearns, S. C., 1976: Life history tactics: A review of the ideas. *Quart. Rev. Biol.,* **51,** 3–47.

Tuljapurkar, S., 1989: An uncertain life: Demography in random environments. *Theor. Population Biol.,* **35,** 227–294.

Vose, R. S., R. L. Schmoyer, P. M. Steurer, T. C. Peterson, R. Heim, T. R. Karl, and J. Eischeid, 1992: The Global Historical Climatology Network: Long-term monthly temperature, precipitation, sea level pressure, and station pressure data. ORNL/CDIAC-53, NDP-041, Carbon Dioxide Information Analysis Center, Oak Ridge National Laboratory, Oak Ridge, TN. [Available from Carbon Dioxide Information Analysis Center, Oak Ridge National Laboratory, P.O. Box 2008, Oak Ridge, TN 37831-6335.]